Pilot and Data Power Control for Scalable Uplink Cell-free massive MIMO

Saeed Mohammadzadeh[1] ***(Member, IEEE)***, **Mostafa Rahmani**[1] ***(Member, IEEE)***, **Kanapathippillai Cumanan,** [1] ***(Senior, IEEE)***, **Alister Burr** [1] ***(Senior, IEEE)***, **AND Pei Xiao** [2] ***(Senior, IEEE)***

[1]School of Physics, Engineering and Technology, University of York, UK
[2]Institute for Communication Systems, University of Surrey, UK

CORRESPONDING AUTHOR: Saeed Mohammadzadeh (e-mail: saeed.mohammadzadeh@york.ac.uk).

The work of Saeed Mohammadzadeh and Kanapathippillai Cumanan was supported by the U.K. Engineering and Physical Sciences Research Council (EPSRC) under Grant EP/X01309X/1

ABSTRACT This paper investigates pilot and data power optimization for cell-free massive MIMO (CF-mMIMO). We propose an iterative algorithm that jointly updates pilot and data power levels to improve channel estimation and ensure reliable data transmission. Pilot powers are allocated based on the normalized mean square error (NMSE) of channel estimation, granting higher power to users with poor estimates while reducing interference for users with favorable conditions. Based on the resulting channel state information (CSI), data powers are then optimized via geometric programming to achieve max–min fairness across users. By alternating between NMSE-driven pilot power control and fairness-oriented data power allocation until convergence, the proposed method achieves efficient CSI acquisition, balanced interference management, and enhanced fairness. In addition, we introduce a lightweight access point (AP)–user association algorithm that ranks AP–user channel strengths, limits the number of users per AP, and employs iterative replacement to ensure scalability and full user connectivity. Simulation results demonstrate that the proposed framework significantly improves spectral efficiency and fairness compared to conventional methods, while remaining suitable for practical CF-mMIMO deployments.

INDEX TERMS AP-user association, pilot and data power control, spectral efficiency, and scalable uplink CF-mMIMO.

I. INTRODUCTION

MOBILE user equipment will keep growing with increasing capacity demands over the next decade, requiring ubiquitous and boundless connectivity. Massive multiple-input multiple-output (mMIMO) is widely recognized as one of the most promising techniques for the 5G and beyond wireless networks, offering significant improvements in spectral efficiency (SE) along with simplified processing and near-optimal performance [1]–[3]. Looking ahead, the main constraints on spectral efficiency (SE) are inter-cell interference due to lack of access point (AP) cooperation, significant path losses, and corresponding hardware energy consumption [4]. Sixth-generation (6G) networks aim to enhance SE by 100 times compared to 5G by addressing these issues with denser, cell-free network infrastructure, transitioning from a cell-centric to a user-centric approach to guarantee comprehensive coverage and high data rate [5].

Unlike traditional cellular networks, CF-mMIMO employs numerous distributed APs equipped with multiple antennas to serve multiple users simultaneously, resulting in significant improvements in coverage, capacity, and reliability [6]–[9].

A. Prior and related works

In CF-mMIMO systems, joint pilot and data power control is a method that simultaneously manages the power levels of both pilot and data signals to optimize overall system performance. By jointly optimizing the allocation of pilot and data powers, we can effectively leverage the spatial diversity of the wireless channel to mitigate key challenges such as pilot contamination, inter-user interference, and noise. Specifically, data power control plays a crucial role in managing inter-user interference, reducing the overlapping interference between users during data transmission. Mean-

while, pilot power control is instrumental in addressing the effects of pilot contamination, enhancing channel estimation accuracy. This dual approach, balancing data and pilot power, enables a more robust and interference-resilient communication environment in CF-mMIMO systems. This problem is challenging to solve because the data power and pilot power optimization problems are non-convex when addressed individually. When combined, they create an even more complex, non-convex optimization problem. Additionally, these two vectors—data power and pilot power—are interdependent, adding another layer of complexity. This interdependence requires careful balancing to achieve an optimal solution that maximizes spectral efficiency while mitigating interference and pilot contamination.

The works in [10]–[12] investigated the effects of the pilot and data PC in the uplink of cell-based systems. However, previous optimization algorithms used in cellular systems cannot be applied to cell-free systems. Each serving AP needs to estimate its wireless channel to its users based on the same uplink pilot signal in cell-free systems. On the other hand, some research on cell-free systems focused on optimizing only the data transmission powers; there is no pilot power control [13], [14] while using full and fixed power to transmit pilot signals.

In [15], an algorithm was proposed based on a pilot power control scheme to minimize the maximum channel estimation error among users. The algorithm used the data power allocation scheme proposed in [13] to solve a max-min fairness problem, while the AP selection is performed based on the largest large-scale fading-based criteria. However, the power levels for both pilot and data signals are not optimized together, meaning their adjustments are not determined simultaneously. The joint power control method was considered in [16] by utilizing single-antenna APs, wherein the users are subject to a limited total energy. The study in [17] proposed a method utilizing first-order optimization to adjust pilot and data power based on a greedy power algorithm. Although the authors describe this approach as joint, it primarily involves sequential optimization of pilot and data power levels rather than fully integrating them. The authors in [18] considered the joint pilot and data power control in user-centric scenarios by combining successive convex approximation and geometric programming (GP). In [19], a sequential convex approximation algorithm is utilized to solve GP to control the pilot and data power jointly. In [20], [21], the authors propose deep learning-based joint pilot and data power control algorithms that address the sum-rate maximization problem. In [22], a pilot allocation scheme based on K-means clustering is developed for CF-mMIMO systems. The work in [23] applies deep learning techniques to design both sum-rate maximization and max–min power allocation strategies. Similarly, the authors of [24] introduce a deep learning-based algorithm to maximize the minimum guaranteed user capacity. In [25], a max–min uplink rate optimization framework is presented, jointly optimizing pilot and data power across all users. The study in [26] proposes a spectral efficiency scheme aimed at maximizing the minimum user rate to enhance fairness in data power optimization. A multi-objective optimization framework is introduced in [27], which effectively addresses the trade-off between fairness and sum spectral efficiency. Furthermore, considering a total energy budget per access point, an optimal power control strategy for allocating pilot and data power is proposed. Authors in [28] employ an unsupervised deep learning approach for uplink power control in CF-mMIMO systems. Moreover, a fractional PC policy for uplink CF-mMIMO was presented in [29], which can be fully distributed and uses large-scale quantities. Inspired by weighted minimum mean square error and fractional programming, the algorithm in [30] proposed a fair power allocation. The authors in [31] introduce an access point-user association strategy combined with pilot power allocation to mitigate multiuser interference and enhance spectral efficiency. Deep neural networks were introduced in [32], [33] to reduce complexity, including convolutional neural network models, distributed DNNs, and graph neural networks for efficient PC optimization with maximum ratio transmission beamforming.

B. Motivation

The deployment of large-scale CF-mMIMO networks demands scalable strategies for both user association and power control. Conventional clustering schemes often lack scalability and fail to guarantee service for all users. Many prior joint designs either optimize pilot and data in a single shot based on fixed channel state information (CSI), or sequentially (pilot-data) without re-optimizing both with updated normalized mean square error (NMSE)/CSI at each iteration. This limits their ability to capture the mutual coupling between estimation quality and interference. These challenges motivate a unified framework that ensures reliable AP–user association and jointly iteratively optimizes pilot and data power, thereby improving scalability, fairness, and overall system performance in practical CF-mMIMO deployments.

C. Contribution

This study introduces a scalable framework for CF-mMIMO that jointly addresses pilot and data power control together with efficient AP–user association. The goal is to ensure both scalability and performance improvement in large-scale deployments.

We first propose an AP–user association algorithm that resolves two key shortcomings of conventional user-centric clustering: the lack of an upper bound on the number of users per AP, which makes the system unscalable as K increases, and the absence of guaranteed association for all users. To address the first issue, we impose a limit on the number of users that each AP can serve. The association process begins by ranking the channel strengths between each AP and all users, after which each AP selects its strongest users

to associate with. This initial step establishes the AP–user association matrix. However, some weaker users may remain unassociated. To ensure full coverage, these users are collected into a separate set and reallocated through an iterative replacement mechanism, where overloaded APs substitute their weakest associated users with unassociated ones. This procedure continues until all users are successfully connected to at least one AP.

We also develop an iterative algorithm that simultaneously adjusts pilot and data power levels to optimize system performance. Each user's signal-to-interference-plus-noise ratio (SINR) is derived under a matched filtering receiver, and the NMSE is formulated as a min–max optimization problem. Since the problem involves non-convex constraints, we employ McCormick relaxation techniques, enabling pilot power to dynamically adapt to instantaneous channel conditions. Based on the resulting CSI and NMSE values, a max–min optimization problem is then solved to allocate data power levels, achieving fairness and reliability in transmission. The key novelty of this design is its iterative structure: pilot powers are updated according to the resulting data power allocations, while data powers are recalculated in response to updated pilot powers. This cycle continues until convergence, ensuring that both pilot and data power vectors evolve jointly. In this way, users with poor channel estimates are allocated higher pilot power to improve estimation accuracy, while users with favorable channel conditions receive lower power to reduce interference and conserve energy. Furthermore, by leveraging geometric programming (GP) techniques [34], [35], data power allocation achieves max–min fairness across users. Unlike previous works [15], [19], which treat pilot and data power optimization separately, the proposed approach integrates them dynamically, ensuring efficient CSI acquisition and effective data transmission simultaneously. Simulation results verify that this iterative strategy substantially improves both spectral efficiency and fairness.

By jointly integrating the iterative pilot–data power control mechanism with the scalable AP–user association strategy, the proposed framework provides a comprehensive solution that ensures efficient power allocation, reliable channel estimation, and scalable user association, making it particularly suitable for practical CF-mMIMO deployments.

D. Outline

The rest of the paper is organized as follows: Section II outlines the system model. In Section III, we propose an iterative power control algorithm that optimizes both pilot and data power allocation to enhance SE. The section also includes the summary and the complexity of the proposed method. Section IV presents simulation results, highlighting the benefits of the proposed method. Finally, Section V concludes the paper.

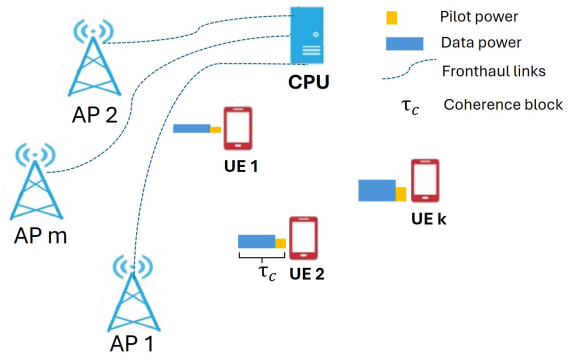

FIGURE 1: Various widths and heights demonstrate different power for pilots and data for different users.

E. Notations

We represent vectors using bold lowercase letters and matrices using bold uppercase letters. $\mathbb{E}\{\cdot\}$ stands for the statistical expectation of random variables, and a circular symmetric complex Gaussian matrix with covariance $\mathbf{Z}$ is denoted by $\mathcal{CN}(0, \mathbf{Z})$. The diagonal matrix is denoted as $\mathrm{diag}(\cdot)$, and the symbol $\mathbb{C}$ is used for the complex numbers. $(\cdot)^{\mathrm{T}}$, $(\cdot)^*$, $(\cdot)^{-1}$, and $(\cdot)^{\mathrm{H}}$ denote transpose, conjugate, inverse, and conjugate-transpose, respectively. The Euclidean norm and absolute value are denoted by $\|\cdot\|$ and $|\cdot|$, respectively. Superscripts $^{\mathrm{p}}$ and $^{\mathrm{d}}$ indicate pilot- and data-related variables or parameters, while $\mathbf{I}$ denotes the identity matrix.

II. System Model

As shown in Fig. 1, we consider a CF-mMIMO system with M randomly distributed APs that serve K single-antenna users, assuming that $K \ll M$. All APs are equipped with N antennas and connected to a CPU via unconstrained fronthaul links. The system operates in time-division duplex mode, and all APs and users are perfectly synchronized. The channel between the m^{th} AP and the k^{th} user is denoted by $\mathbf{g}_{mk} \in \mathbb{C}^N$. In each block, an independent realization from a correlated Rayleigh fading distribution is drawn:

$$\mathbf{g}_{mk} \sim \mathcal{CN}(0, \mathbf{R}_{mk}) \tag{1}$$

where $\mathbf{R}_{mk} = \mathrm{tr}(\mathbf{R}_{mk})/N$ is the large-scale fading that describes geometric pathloss and shadowing, and $\mathbf{R}_{mk} = \mathbb{E}\{\hat{\mathbf{g}}_{mk}\hat{\mathbf{g}}_{mk}^{\mathrm{H}}\}$. We assume that at each of the m^{th} AP, the local statistical channel state information (CSI) of all connected links is perfectly known, as it can be estimated using standard methods [36]. We consider a system that operates in the block-fading channel model, where the time and frequency plane is divided into coherence blocks, τ_c, in which τ_p and $\tau_c - \tau_p$ dedicate the uplink pilot, and data transmission symbols, respectively.

A. Uplink Training and Channel Estimation

In this paper, we consider a CF-mMIMO network where a subset of APs in the network serves each user. We assume

that each user selects its pilot sequence randomly, which can be conducted in a fully distributed manner. Since the number of symbols for the training is τ_p, only τ_p orthogonal pilot sequences are available in the network, so for $K > \tau_p$, multiple users have to share the same pilot sequence. This random pilot assignment approach is straightforward but often results in nearby users sharing the same pilot sequence. Consequently, these users experience degraded performance due to substantial pilot contamination effects. The focus of this paper is not based on the pilot decontamination algorithm, and we assume significant pilot contamination in this study due to random pilot assignment, allowing us to evaluate the proposed method under worst-case conditions.

We consider τ_p mutually orthogonal pilot sequences $\{\boldsymbol{\phi}_1, \ldots, \boldsymbol{\phi}_{\tau_p}\}$, each of length τ_p and normalized such that $\|\boldsymbol{\phi}_t\|^2 = \tau_p$. The value of τ_p is fixed and does not scale with the number of UEs K. Each UE is assigned one of these pilots upon access. In practical massive access scenarios where $K > \tau_p$, multiple UEs inevitably reuse the same pilot. These UEs are referred to as pilot-sharing UEs. Let $t_k \in \{1, \ldots, \tau_p\}$ denote the pilot index of UE k, and define $\mathcal{S}_k \subseteq \{1, \ldots, K\}$ as the set of UEs reusing pilot t_k, including UE k itself. When the UEs in $\mathcal{S}_k$ transmit the shared pilot $\boldsymbol{\phi}_{t_k}$, the received signal at AP m, denoted by $\mathbf{y}^{\mathrm{p}}_{m_{t_k}} \in \mathbb{C}^N$, can be written as [37, Sec. 3]

$$\mathbf{y}^{\mathrm{p}}_{m_{t_k}} = \sum_{i \in \mathcal{S}_k} (\tau_p p_i^{\mathrm{p}})^{1/2} \mathbf{g}_{mi} + \mathbf{n}_{m_{t_k}} \tag{2}$$

where p_i^{p} denotes the pilot transmit power of UE i and $\mathbf{n}_{m_{t_k}} \sim \mathcal{N}_{\mathbb{C}}\left(\mathbf{0}, \sigma^2 \mathbf{I}_N\right)$ is the thermal noise. The MMSE estimate of $\mathbf{g}_{mk}$ for $k \in \mathcal{S}_k$ is given by

$$\hat{\mathbf{g}}_{mk} = (\tau_p p_k^{\mathrm{p}})^{1/2} \mathbf{R}_{mk} \boldsymbol{\Theta}^{-1}_{m_{t_k}} \mathbf{y}^{\mathrm{p}}_{m_{t_k}} \tag{3}$$

where $\mathbf{B}_{mk} = \mathbb{E}\left\{\hat{\mathbf{g}}_{mk} \hat{\mathbf{g}}^{\mathrm{H}}_{mk}\right\} = \tau_p p_k^{\mathrm{p}} \mathbf{R}_{mk} \boldsymbol{\Theta}^{-1}_{m_{t_k}} \mathbf{R}_{mk}$, and

$$\boldsymbol{\Theta}_{m_{t_k}} = \mathbb{E}\{\mathbf{y}^{\mathrm{p}}_{m_{t_k}} (\mathbf{y}^{\mathrm{p}}_{m_{t_k}})^{\mathrm{H}}\} = \sum_{i \in \mathcal{S}_k} \tau_p p_i^{\mathrm{p}} \mathbf{R}_{mi} + \sigma^2 \mathbf{I}_N \tag{4}$$

The interference caused by the pilot-sharing users in $\mathcal{S}_t$ as indicated in (2) leads to pilot contamination, which degrades the system performance. Therefore, pilot contamination degrades the estimation performance, making coherent transmission less effective, and the estimates $\hat{\mathbf{g}}_{mk}$ for $k \in \mathcal{S}_t$ become correlated, leading to additional interference [37].

B. Uplink Data Transmission and Achievable SE

During the uplink data transmission, all users send their data to the APs using the same time-frequency resource. The received signal $\mathbf{y}^{\mathrm{d}}_m \in \mathbb{C}^N$, at the m^{th} AP is given by

$$\mathbf{y}^{\mathrm{d}}_m = \sum_{k=1}^{K} (p_k^{\mathrm{d}})^{1/2} \mathbf{g}_{mk} q_k + \mathbf{w}^{\mathrm{d}}_m, \tag{5}$$

where p_k^{d} is the transmit data power, q_k with $\mathbb{E}\{|q_k|^2|\} = 1$, is the data symbol transmitted by k^{th} user, and $\mathbf{w}^{\mathrm{d}}_m \in \mathcal{CN}(0, \sigma^2 \mathbf{I}_N)$ is the additive white Gaussian noise at the receiver. For signal detection in the first stage, the m^{th} AP utilizes the maximum ratio combining (MRC) technique in which the received signal, $\mathbf{y}^{\mathrm{d}}_m$ is multiplied by the Hermitian transpose of channel estimate, $\hat{\mathbf{g}}^{\mathrm{H}}_{mk}$ and transmits $\hat{\mathbf{g}}^{\mathrm{H}}_{mk} \mathbf{y}^{\mathrm{d}}_m$ to the CPU through the backhaul link for all users. Then, for each user, k, the received products are combined as

$$\begin{aligned} y_k = \sum_{m=1}^{M} \hat{\mathbf{g}}^{\mathrm{H}}_{mk} \mathbf{y}^{\mathrm{d}}_m &= (p_k^{\mathrm{d}})^{1/2} \Big(\sum_{m=1}^{M} \hat{\mathbf{g}}^{\mathrm{H}}_{mk} \mathbf{g}_{mk} \Big) q_k \\ &+ \sum_{\substack{i=1 \\ i \neq k}}^{K} (p_i^{\mathrm{d}})^{1/2} \Big(\sum_{m=1}^{M} \hat{\mathbf{g}}^{\mathrm{H}}_{mk} \mathbf{g}_{mi} \Big) q_i + w'_k, \end{aligned} \tag{6}$$

where $w'_k = \sum_{m=1}^{M} \hat{\mathbf{g}}^{\mathrm{H}}_{mk} \mathbf{w}^{\mathrm{d}}_m$ represents the noise. In the second stage, the CPU gathers the local data estimates from all APs and combines them to create a final estimate of the user data. The CPU calculates its estimate using a linear combination of the local estimates as

$$\begin{aligned} \hat{y}_k &= \sum_{m=1}^{M} a^*_{mk} \hat{\mathbf{g}}^{\mathrm{H}}_{mk} \mathbf{y}^{\mathrm{d}}_m \\ &= (p_k^{\mathrm{d}})^{1/2} \Big(\sum_{m=1}^{M} a^*_{mk} \hat{\mathbf{g}}^{\mathrm{H}}_{mk} \mathbf{g}_{mk} \Big) q_k \\ &+ \sum_{\substack{i=1 \\ i \neq k}}^{K} (p_i^{\mathrm{d}})^{1/2} \Big(\sum_{m=1}^{M} a^*_{mk} \hat{\mathbf{g}}^{\mathrm{H}}_{mk} \mathbf{g}_{mi} \Big) q_i + w''_k, \end{aligned} \tag{7}$$

where $w''_k = \sum_{m=1}^{M} a^*_{mk} \hat{\mathbf{g}}^{\mathrm{H}}_{mk} \mathbf{w}^{\mathrm{d}}_m$ and $a_{mk} \in \mathbb{C}$ defines the weight assigned by the CPU to the local signal estimate that the m^{th} AP has of the signal from the k^{th} user. In this paper, we have assumed that the large-scale fading weight vector of user k for all APs is deterministic.

For simplicity, we define the vector $\mathbf{u}_{jk} \in \mathbb{C}^M$ formed as

$$\mathbf{u}_{ik} = [\hat{\mathbf{g}}^{\mathrm{H}}_{1k} \mathbf{g}_{1i}, \cdots, \hat{\mathbf{g}}^{\mathrm{H}}_{Mk} \mathbf{g}_{Mi}]^T, \tag{8}$$

where it represents the vector containing the combined receive channels between i^{th} user and all APs serving k^{th} user. Using (8), the received signal at k^{th} user in (7) can be expressed as

$$\hat{y}_k = (p_k^{\mathrm{d}})^{1/2} \mathbf{a}_k^{\mathrm{T}} \mathbf{u}_{kk} q_k + \sum_{\substack{i=1 \\ i \neq k}}^{K} (p_i^{\mathrm{d}})^{1/2} \mathbf{a}_k^{\mathrm{T}} \mathbf{u}_{ik} q_i + w''_k. \tag{9}$$

where $\mathbf{a}_k = [a_{1k}, \cdots, a_{mk}, \cdots, a_{Mk}]^{\mathrm{T}}$. It can be observed from (9) that the effective channels of the different users are represented by $(\mathbf{a}_k \mathbf{u}_{ik} : i = 1, \cdots, K)$, as it has the structure of a single antenna channel. In order to compute the SE, we assume that the average of the effective channel, $\mathbb{E}\{\mathbf{a}_k \mathbf{u}_{kk}\}$ is non-zero and deterministic, even though the effective channel $\mathbf{a}_k \mathbf{u}_{kk}$ is unknown at the CPU [38]. Then, it can be assumed to be known. Therefore, the achievable uplink SE of the k^{th} user can be written as follows

$$\mathrm{SE}_k = (1 - \frac{\tau_p}{\tau_{\mathrm{c}}}) \log_2 (1 + \mathrm{SINR}_k), \tag{10}$$

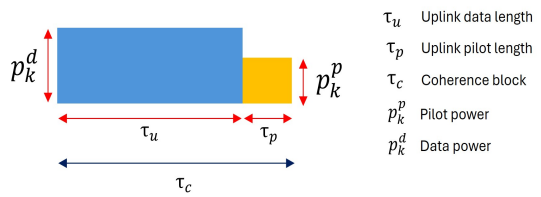

FIGURE 2: Demonstration of pilot and data power allocation based on τ_p and $\tau_u = \tau_c - \tau_p$ for uplink

where the SINR of the k^{th} user is presented by [39]

$$\text{SINR}_k = \frac{p_k^{\text{d}} \left|\mathbf{a}_k \mathbb{E}\{\mathbf{u}_{kk}\}\right|^2}{\mathbf{a}_k^{\text{T}} \left(\sum_{i=1}^{K} p_i^{\text{d}} \mathbb{E}\{\mathbf{u}_{ik}\mathbf{u}_{ik}^{\text{H}}\} - p_k^{\text{d}} \mathbb{E}\{\mathbf{u}_{kk}\}\mathbb{E}\{\mathbf{u}_{kk}^{\text{H}}\} + \mathbf{F}_k \right) \mathbf{a}_k}, \tag{11}$$

where $\mathbf{a}_k = [1, \cdots, 1]^{\text{T}} \in \mathbb{R}^M$ and

$$[\mathbb{E}\{\mathbf{u}_{ki}\}]_m = \begin{cases} \sigma^2 p_k^{\text{p}} \tau_p \ \text{tr}(\mathbf{R}_{mk} \Theta_{mk}^{-1} \mathbf{R}_{mk}) & i \in \mathcal{S}_k, \\ 0 & i \notin \mathcal{S}_k \end{cases}, \tag{12}$$

$$[\mathbf{F}_k]_{mm} = \sigma^2 p_k^{\text{p}} \tau_p \ \text{tr}(\mathbf{R}_{mk} \Theta_{mk}^{-1} \mathbf{R}_{mk}) \tag{13}$$

$$[\mathbb{E}\{\mathbf{u}_{ik}\mathbf{u}_{ik}^{\text{H}}\}]_{mm} = \tau_p p_k^{\text{p}} \text{tr}(\mathbf{R}_{mi} \mathbf{R}_{mk} \Theta_{mk}^{-1} \mathbf{R}_{mk}) + \begin{cases} p_k^{\text{p}} p_i^{\text{p}} \tau_p^2 \left|\text{tr}(\mathbf{R}_{mi} \Theta_{mk}^{-1} \mathbf{R}_{mk})\right|^2 & i \in \mathcal{S}_k, \\ 0 & i \notin \mathcal{S}_k \end{cases} \tag{14}$$

C. Scalability

In order to address the scalability of CF-mMIMO, we propose a framework that ensures scalable operation by introducing a block-diagonal matrix $\mathbf{L}$. This matrix is composed of diagonal sub-matrices $\mathbf{L}_{mi} \in \mathbb{C}^{N \times N}$, where $i = 1, \ldots, K$ denotes the user index and $m = 1, \ldots, M$ denotes the AP index. The role of $\mathbf{L}_{mi}$ is to indicate which antennas of AP m are assigned to serve user i. Specifically, if the q-th antenna of AP m is configured to transmit to or decode the signal from user i, then the q-th diagonal entry of $\mathbf{L}_{mi}$ is set to 1, and 0 otherwise. To further characterize the AP–user associations, a binary matrix $\mathbf{T} \in \mathbb{R}^{M \times K}$ is defined, where the entry $\mathbf{T}_{mk}$ equals 1 if the sum of diagonal elements of $\mathbf{L}_{mk}$ is nonzero, and 0 otherwise. Based on this definition, the subset of users associated with AP m is given by

$$\mathcal{M}_m = \{i \mid \mathbf{T}_{mi} = 1, \ i = 1, \ldots, K\},$$

and the subset of APs associated with user k is expressed as

$$\mathcal{A}_k = \{m \mid \mathbf{T}_{mk} = 1, \ m = 1, \ldots, M\}.$$

D. AP-user association

We first develop an AP–user association algorithm that addresses two major limitations of the conventional user-centric clustering approach: (i) the absence of an upper bound on the number of users that can associate with a single AP, which compromises scalability as K increases, and (ii) the lack of a guarantee that all users are associated with at least one AP.

Following the assumption in [40, Sec. V], we impose a maximum limit of τ_p users per AP, i.e.,

$$|\mathcal{M}_m| \leq \tau_p, \quad m = 1, \ldots, M,$$

to mitigate the first limitation.

The proposed algorithm proceeds as follows. For each AP m, the large-scale fading coefficients with all users are sorted in descending order. AP m then selects the first τ_p users for association. This procedure is repeated for all APs, after which the AP–user association matrix $\mathbf{T}$ is constructed. However, since the initial association prioritizes users with stronger large-scale fading, weaker users may remain unassociated.

To ensure universal association, the algorithm identifies such weak users and groups them into a set $\mathcal{W}$. A replacement mechanism is then applied iteratively:

1. The AP i with the maximum cumulative β across its associated users, $\mathcal{M}_i$, is identified.
2. Within $\mathcal{M}_i$, the user j with the weakest channel is selected, i.e.,

$$j = \underset{k \in \mathcal{M}_i}{\text{argmin}} \ \mathbf{g}_{ik}.$$

3. User j is replaced with the first user from the weak-user set $\mathcal{W}$.

This replacement procedure is repeated until $\mathcal{W} = \emptyset$, thereby ensuring that every user is associated with at least one AP. In this way, the proposed algorithm guarantees both scalability and full coverage in the AP–user association process.

III. Proposed pilot and data power control

In this section, we introduce the pilot and data power control technique. It determines the transmission power allocated by each user and the proportion of this power dedicated to pilot signals and data transmission. To this end, we introduce a novel constraint based on the maximum transmit budget power for the user and the coherence block and develop an iterative algorithm to minimize the NMSE. Subsequently, we employ a scheme based on McCormick relaxation to adjust the pilot power according to real-time channel conditions. Following this, we use GP to solve the max-min fairness

$$\text{SINR}_k = \frac{p_k^{\text{d}} p_k^{\text{p}} \tau_p \, \text{tr}(\mathbf{R}_{mk} \boldsymbol{\Theta}_{m_{t_k}}^{-1} \mathbf{R}_{mk})}{\sum_{i=1}^{K} \frac{p_i^{\text{d}} \, \text{tr}(\mathbf{R}_{mi} \mathbf{R}_{mk} \boldsymbol{\Theta}_{m_{t_k}}^{-1} \mathbf{R}_{mk})}{\text{tr}(\mathbf{R}_{mk} \boldsymbol{\Theta}_{m_{t_k}}^{-1} \mathbf{R}_{mk})} + \sum_{\substack{i \in \mathcal{S}_k \\ i \neq k}} \frac{p_i^{\text{p}} p_k^{\text{d}} \tau_p |\, \text{tr}(\mathbf{R}_{mi} \boldsymbol{\Theta}_{m_{t_k}}^{-1} \mathbf{R}_{mk})|^2}{\text{tr}(\mathbf{R}_{mk} \boldsymbol{\Theta}_{m_{t_k}}^{-1} \mathbf{R}_{mk})} + \sigma^2} \tag{15}$$

optimization problem and allocate data power for each user. The algorithm aims to maximize the system's performance, including spectral efficiency and fairness, while adhering to specific constraints, such as total transmit power. Notably, this methodology differs from others by iteratively updating and adjusting both power levels for each channel realization.

A. Pilot and data power assignment

In CF-mMIMO, determining the per-user maximum transmit energy depends on system requirements like spectral efficiency, coherence block length, and interference management. Generally, the maximum transmit budget per user (often denoted as P_{max}) is determined based on the hardware's power budget, regulatory constraints, and the need to mitigate interference. Studies suggest optimal power control strategies, including fractional or adaptive transmit power adjustments, help maintain performance within the system's maximum energy limits, balancing data and pilot power for reduced interference and improved coverage. Thus, we can write

$$\tau_p p_k^{\text{p}} + (\tau_c - \tau_p) p_k^{\text{d}} \leq E_{\text{max}} \Rightarrow \frac{\tau_p p_k^{\text{p}} + (\tau_c - \tau_p) p_k^{\text{d}}}{\tau_c} \leq P_{\text{max}}. \tag{16}$$

where $E_{\text{max}} = \tau_c P_{\text{max}}$. This inequality implies that pilot power (p_k^{p}) and data power (p_k^{d}) are jointly constrained to ensure the total average transmit power remains within P_{max}. This relationship allows the system to manage the balance between pilot training and data transmission within the coherence block, which is important for improving spectral efficiency and mitigating interference. Fig. 2 illustrates the allocation of pilot and data power based on the pilot sequence τ_p and the coherence block duration, τ_c. This figure serves as a heuristic example aimed at providing an intuitive understanding of the scenario under consideration rather than offering a rigorous analysis.

On the other hand, the coherence block duration, τ_c is influential in determining how transmit power is allocated in communication systems, particularly in multi-user scenarios. Although a user's transmit power is constrained by its hardware, such as amplifier efficiency and power limits, the coherence block length indirectly affects how efficiently this power can be used. Longer coherence blocks allow for more data symbols per channel estimation, enhancing spectral efficiency by reducing the time spent on training. In contrast, shorter coherence blocks, caused by high mobility or challenging environments, require more frequent re-estimation, limiting the potential efficiency for a given power budget. Additionally, shorter coherence durations make managing inter-user interference more complex, often requiring higher power levels to maintain service quality. Therefore, the duration of the coherence block can impact the power control strategies, ultimately influencing overall system performance. Moreover, the significance of τ_p is to quantify how much energy each terminal spends on pilots in each coherence interval [41].

Based on this information, our objective in the following section is to utilize two distinct constraints—one for pilot power and the other for data power:

$$p_k^{\text{p}} \leq \frac{\tau_c P_{\text{max}} - (\tau_c - \tau_p) p_k^{\text{d}}}{\tau_p}, \tag{17}$$

$$p_k^{\text{d}} \leq \frac{\tau_c P_{\text{max}} - \tau_p p_k^{\text{p}}}{(\tau_c - \tau_p)}. \tag{18}$$

These constraints are designed to ensure efficient resource allocation while maintaining system performance. The pilot power constraint will address the proper power allocation for channel estimation, minimizing interference, and ensuring accurate channel state information. Meanwhile, the data power constraint will optimize the power used for data transmission to enhance spectral efficiency and mitigate interference. Together, these constraints form the foundation for a robust power control strategy tailored to the system's requirements.

B. Pilot Power control

During the training phase, the AP estimates the channels using the user pilots. However, due to non-orthogonality among pilot sequences, a pilot signal from one user can adversely affect the channel estimate of other users. This is known as the pilot contamination effect and can be particularly severe in CF-mMIMO systems that aim to serve multiple users simultaneously with the same time-frequency resource. Therefore, it is crucial to mitigate pilot contamination. To this end, we introduce iterative pilot power coefficients that can improve channel estimation accuracy during the training phase.

It is known that the average channel gain influences the MSE value. Although a stronger channel may exhibit larger absolute errors than a weaker channel, the relative size of the error is more critical than its absolute magnitude. Consequently, estimation accuracy is evaluated using the NMSE. Specifically, for the channel between the m^{th} AP and the k^{th} user, the NMSE is defined as [38]:

$$\begin{aligned} \text{NMSE}_{mk} &= \frac{\mathbb{E}\{\|\mathbf{g}_{mk} - \hat{\mathbf{g}}_{mk}\|^2\}}{\mathbb{E}\{\|\mathbf{g}_{mk}\|^2\}} \\ &= 1 - \frac{p_k^{\text{p}} \tau_p \text{tr}(\mathbf{R}_{mk} \Theta_{mk}^{-1} \mathbf{R}_{mk})}{\text{tr}(\mathbf{R}_{mk})}. \end{aligned} \tag{19}$$

The system calculates the variance of the channel estimation error between the m^{th} AP and the k^{th} user and presents it as a relative value. It can be seen from (19) that NMSE reduces as the channel estimation error ($\mathbf{g}_{mk} - \hat{\mathbf{g}}_{mk}$) of the k^{th} user decreases. The proposed algorithm aims to allocate pilot power for each user and provide uniformly good service to all network users. We formulate a min-max optimization problem designed to minimize the maximum user-NMSE based on a novel constraint based on the maximum transmit budget at the users and the coherence time to achieve this

objective as follows

$$\mathbf{P1}: \min_{\{p_k^{\mathrm{p}}\}} \max_{k=1,\ldots,K} \sum_{m\in\mathcal{A}_k} \mathrm{NMSE}_{mk}$$
$$\text{s.t.} \quad p_k^{\mathrm{p}} \le \frac{\tau_c P_{\max} - (\tau_c-\tau_p)p_k^{\mathrm{d}}}{\tau_p} \tag{20a}$$
$$\epsilon \le p_k^{\mathrm{p}}, \quad \forall k \in \mathcal{K} \tag{20b}$$

where $P_{\max}$ denotes the maximum transmit budget available for each user. Constraint (20a) maintains a balance between the power assigned for pilot and data transmission, allowing the total power usage to stay within the prescribed limits. The inequality reflects a trade-off between utilizing power for pilot transmission to estimate channel parameters and allocating power for data transmission for information transfer. To solve the optimization problem in (20). without loss of generality, problem **P1** can be rewritten by introducing a new slack variable as

$$\mathbf{P2}: \min_{\{p_k^{\mathrm{p}},\nu\}} \nu$$
$$\text{s.t.}$$
$$\sum_{m\in\mathcal{A}_k} \left(1 - \frac{p_k^{\mathrm{p}}\tau_p \mathrm{tr}(\mathbf{R}_{mk}\Theta_{mk}^{-1}\mathbf{R}_{mk})}{\mathrm{tr}(\mathbf{R}_{mk})}\right) \le \nu \tag{21a}$$
$$\epsilon \le p_k^{\mathrm{p}} \le \frac{\tau_c P_{\max} - (\tau_c-\tau_p)p_k^{\mathrm{d}}}{\tau_p}, \quad \forall k \in \mathcal{K} \tag{21b}$$

However, the constraint involving the sum of ratios in (21a) is non-convex due to the division by a quadratic term. Thus, problem **P2** is non-convex. To tackle this non-convexity, we present a computationally efficient algorithm to convert the concave constraint into a convex one based on McCormick relaxation. This technique introduces auxiliary variables and linear constraints to approximate the concave term with a piecewise linear function. The McCormick relaxation algorithm is utilized to address non-convex optimization problems by creating convex and concave relaxations to approximate the non-convex feasible region. We rewrite (21a) as

$$1 - \frac{p_k^{\mathrm{p}}\tau_p \ \mathrm{tr}(\mathbf{R}_{mk}\Theta_{mk}^{-1}\mathbf{R}_{mk})}{\mathrm{tr}(\mathbf{R}_{mk})} = q_{mk}. \quad \forall m,k \tag{22}$$

To linearize this term using McCormick relaxation, we can introduce auxiliary variables z_{mk} and v_{mk} to approximate q_{mk}:

$$z_{mk} = \mathrm{tr}(\mathbf{R}_{mk}), \tag{23}$$
$$v_{mk} = p_k^{\mathrm{p}}\tau_p \ \mathrm{tr}(\mathbf{R}_{mk}\Theta_{mk}^{-1}\mathbf{R}_{mk}), \tag{24}$$

where $z_{mk} \ge 0$ and $v_{mk} \ge 0$. We then add linear constraints to ensure that z_{mk} and v_{mk} correctly approximate q_{mk}, and we reformulate the optimization problem as follows:

$$\mathbf{P3}: \min_{\{p_k^{\mathrm{p}},\nu\}} \nu$$
$$\text{s.t.} \quad \sum_{m\in\mathcal{A}_k} q_{mk} \le \nu \tag{25}$$
$$q_{mk} \le 1 - \frac{z_{mk}}{v_{mk}} + (1 - z_{mk})$$
$$q_{mk} \ge 1 - \frac{z_{mk}}{v_{mk}} + (1 - v_{mk})$$
$$\epsilon \le p_k^{\mathrm{p}} \le \frac{\tau_c P_{\max} - (\tau_c-\tau_p)p_k^{\mathrm{d}}}{\tau_p}, \quad \forall k \in \mathcal{K}$$

This method allows for the creation of relaxations that can be solved efficiently and provide bounds for the optimal solution. These constraints and the objective function represent the linearized form of the original non-convex optimization problem **P2**. Thus, problem **P1** can be solved by solving a sequence of convex problems **P3**. Using yet another linear matrix inequalities parser (YALMIP) [42] of Matlab toolbox, the optimized result is represented by the pilot power vector $\hat{\mathbf{p}}_k^{\mathrm{p}}$, which stacks all pilot power coefficients $\hat{p}_k^{\mathrm{p}}$.

C. Data Power Control

One important aspect of CF-mMIMO systems is their capability to provide consistently equal service to all users. We focus on the optimization problem of max-min fairness, which entails using the pilot power coefficients calculated in problem **P3**, ($\hat{\mathbf{p}}_k^{\mathrm{p}}$), and optimizing the data power control coefficient to maximize the minimum user rates. We denote the data power coefficient vector as $\mathbf{p}_k^{\mathrm{d}} = [p_1^{\mathrm{d}}, p_2^{\mathrm{d}}, \cdots, p_K^{\mathrm{d}}]$, then rewrite the uplink SE of k^{th} user as

$$\mathrm{SE}_k(\hat{\mathbf{p}}_k^{\mathrm{p}}, \mathbf{p}_k^{\mathrm{d}}) = (1 - \frac{\tau_p}{\tau_c}) \log_2\left(1 + \mathrm{SINR}_k(\hat{\mathbf{p}}_k^{\mathrm{p}}, \mathbf{p}_k^{\mathrm{d}})\right), \tag{26}$$

and optimization problem is formulated as:

$$\mathbf{P4}: \max_{\{p_k^{\mathrm{d}}\}} \min_{k=1,\ldots,K} \mathrm{SE}_k(\hat{\mathbf{p}}_k^{\mathrm{p}}, \mathbf{p}_k^{\mathrm{d}})$$
$$\text{s.t.} \quad 0 \le p_k^{\mathrm{d}} \le \frac{\tau_c P_{\max} - \tau_p \hat{p}_k^{\mathrm{p}}}{(\tau_c - \tau_p)}, \quad \forall k \in \mathcal{K} \tag{27}$$

We exploit GP (convex problem) to develop an efficient solution for Problem **P4**, which is defined in (27). Problem **P4** cannot be directly solved through the optimization software. By utilizing the slack variables, the optimization problem can be reformulated as

$$\mathbf{P5} \quad \max_{\{p_k^{\mathrm{d}}\},t} t$$
$$\text{s.t.} \quad t \le \mathrm{SINR}_k(\hat{\mathbf{p}}_k^{\mathrm{p}}, \mathbf{p}_k^{\mathrm{d}}), \tag{28a}$$
$$0 \le p_k^{\mathrm{d}} \le \frac{\tau_c P_{\max} - \tau_p \hat{p}_k^{\mathrm{p}}}{(\tau_c - \tau_p)}, \quad \forall k \in \mathcal{K}, \tag{28b}$$

To tackle this optimization problem and explicitly expand the SINR_k expression in (11), we focus on the special case of spatially uncorrelated fading, i.e., $\mathbf{R}_{mk} = \beta_{mk}\mathbf{I}_N$. Under

this assumption, (11) simplifies as

$$\frac{N\tau_p p_k^{\mathrm{d}} p_k^{\mathrm{p}} \sum_{m\in\mathcal{A}_k} \beta_{mk}^2 \theta_m^{-1}}{\sum_{m\in\mathcal{A}_k}\left(N\tau_p \sum_{\substack{i\in\mathcal{S}_k \\ i\neq k}} p_i^{\mathrm{d}} p_i^{\mathrm{p}} \beta_{mi}^2 \theta_m^{-1} + \sum_{i=1}^{K} p_i^{\mathrm{d}} \beta_{mi}\right) + \sigma^2}, \tag{29}$$

where $\theta_m = \tau_p \sum_{i\in\mathcal{S}_k} p_i^{\mathrm{p}} \beta_{mi} + \sigma^2$.

Lemma 1. *Problem 5 (**P5**) can be solved using a GP, allowing for a globally optimal solution in polynomial time.*

Proof: Problem (28) can be written as a GP in standard form [42]. In (28), the objective function is already in the form of t, a monomial and thus a valid posynomial[1] The power constraints are expressed as monomials, while the SINR expressions can be rearranged as posynomial constraints as follows in Appendix B.

Additionally, equation (28b) is in the form of a posynomial. Since geometric programs have a convex structure, **P5** can be efficiently solved in a centralized manner using the interior-point toolbox CVX [42], [43]. This process must be repeated until the maximum number of iterations is reached. The proposed method is summarized in step 2 of the Algorithm 1.

The transmitted data power allocated to user k is intricately influenced by several key factors. Firstly, the maximum transmit power, denoted by $P_{\max}$, sets a fundamental constraint on the power level that can be allocated to each user. Additionally, the coherence block duration, represented by τ_c, is pivotal in determining the permissible power allocation. This duration governs the temporal coherence of the channel, thereby influencing the power allocation strategy. Moreover, the estimated pilot power, denoted by $\hat{p}_k^{\mathrm{p}}$, is a crucial parameter calculated based on the minimization of the normalized mean square error for the channel. This estimation process ensures an optimal trade-off between pilot power and channel estimation accuracy, directly impacting the effectiveness of the power allocation scheme. Collectively, these factors underscore the intricate interplay between system parameters and optimization objectives in determining the transmitted data power for each user.

The key distinction between the proposed method and existing algorithms lies in their approach to updating data power based on channel states. Unlike most prior works—including single-shot joint formulations and sequential schemes—we alternate NMSE-driven pilot power updates with fairness-oriented data power optimization, feeding back the updated CSI/NMSE each round. This explicitly models the interdependence between estimation accuracy and interference. Specifically, existing approaches often compute pilot power independently and subsequently utilize it to determine data power. In contrast, our proposed method directly incorporates CSI into the data power calculation. By considering the variance of the channel in which the pilot power is utilized, our approach offers a more integrated and adaptive strategy for power allocation, potentially leading to improved system performance and efficiency.

[1]A function $q\left(y_1,\ldots,y_{T_1}\right) = \sum_{t=1}^{T_2} a_t \prod_{m=1}^{T_1} y_m^{b_{t,m}}$ is posynomial with T_2 terms ($T_2 \geq 2$) if the coefficients $b_{t,m}$ are real numbers and the coefficients a_t are nonnegative real numbers. When $T_2 = 1, q\left(y_1,\ldots,y_{T_1}\right)$ is a monomial.

Algorithm 1: Proposed Scalable Power Optimization

Input: Set of APs $\mathcal{M}$, users $\mathcal{K} = \{1,\ldots,K\}$, $\mathbf{h}_{mk}$ for all $m \in \mathcal{M}, k \in \mathcal{K}$;
Initialization: $\mathbf{p}_k^{\mathrm{d}} = [1,\ldots,1]$, $\boldsymbol{\zeta} > 0$;
Step 1: AP–User Association (Scalable Framework) ;
Construct the block-diagonal matrix $\mathbf{L}$ with sub-matrices $\mathbf{L}_{mi}$ to indicate antenna allocation for AP m and user i;
Build the binary AP–user association matrix $\mathbf{T}$ where $\mathbf{T}_{mk} = 1$ if $\sum \mathrm{diag}(\mathbf{L}_{mk}) > 0$;
for *each AP* m **do**
    Sort $\{\mathbf{R}_{mk}, k = 1,\ldots,K\}$ in descending order;
    Select the top τ_p users to form the set $\mathcal{M}_m$ (enforcing $|\mathcal{M}_m| \leq \tau_p$);
end
Identify unassociated weak users and group them into $\mathcal{W}$;
while $\mathcal{W} \neq \emptyset$ **do**
    Find AP $i = \arg\max_m \sum_{k\in\mathcal{M}_m} \mathbf{h}_{mk}$;
    Find weakest user $j = \arg\min_{k\in\mathcal{M}_i} \mathbf{h}_{ik}$;
    Replace j with first element in $\mathcal{W}$ and update $\mathbf{T}$;
    Remove that user from $\mathcal{W}$;
end
Obtain $\mathcal{A}_k = \{m \mid \mathbf{T}_{mk} = 1,\ m = 1,\ldots,M\}$;
Step 2: Iterative Power Optimization ;
for *each channel realization* **do**
    repeat
        Solve Problem **P3** (25) (pilot power optimization) $\rightarrow \hat{\mathbf{p}}_k^{\mathrm{p}}$;
        Update $\mathrm{SINR}_k(\hat{\mathbf{p}}_k^{\mathrm{p}}, \mathbf{p}_k^{\mathrm{d}})$ in (28a) using (15);
        Update constraint in (28b) ;
        Solve Problem **P5** (28) (data power optimization) $\rightarrow \hat{\mathbf{p}}_k^{\mathrm{d_{new}}}$;
    until *convergence*;
    if $\|\hat{\mathbf{p}}_k^{\mathrm{d}_{new}} - \hat{\mathbf{p}}_k^{\mathrm{d}_{old}}\| > \boldsymbol{\zeta}$ **then**
        $\hat{\mathbf{p}}_k^{\mathrm{d}^*} = \hat{\mathbf{p}}_k^{\mathrm{d_{new}}}$; **break**;
    else
        $\hat{\mathbf{p}}_k^{\mathrm{d_{old}}} = \hat{\mathbf{p}}_k^{\mathrm{d_{new}}}$; go to Line 21;
    end
end
Output: $\hat{\mathbf{p}}_k^{\mathrm{d}^*}$, $\hat{\mathbf{p}}_k^{\mathrm{p}^*}$;
for *each user* k **do**
    Compute SINR_k from (15);
    Compute SE_k from (26);
end
Final Output: Achieved $\mathrm{SE} = \{\mathrm{SE}_1,\ldots,\mathrm{SE}_K\}$;

IV. Computational Complexity

To evaluate the computational requirements, we compute the complexity of each component for K users and $|\mathcal{A}_k| \leq M$ APs within the power control methods in terms of floating point operations (FLOPs) as follows. The computational complexity of the proposed iterative pilot power allocation (IPPA) method is explained in Algorithm 1, which solves the problem **P3** and the GP convex optimization problem, **P5** at each iteration. For pilot power calculation, we consider **P3**. The calculation process for q_{mk} includes z_{mk} with complexity of $\mathcal{O}(|\mathcal{A}_k|K)$ and v_{mk} with complexity of $\mathcal{O}(2|\mathcal{A}_k|K\tau_p^2)$. At the same time, the division makes $\mathcal{O}(2|\mathcal{A}_k|K)$ and summation for each k is $\mathcal{O}(|\mathcal{A}_k|K)$. On the other hand, constraints have totally $\mathcal{O}(6|\mathcal{A}_k|K^2)$. Thus, the totals complexity for solving **P3** is $\mathcal{O}(2|\mathcal{A}_k|K\tau_p^2+|\mathcal{A}_k|K+2|\mathcal{A}_k|K+K|\mathcal{A}_k|+6|\mathcal{A}_k|K^2) \approx \mathcal{O}(2|\mathcal{A}_k|K\tau_p^2+6|\mathcal{A}_k|K^2)$. For the data power optimization problem in **P5**, calculating SINR across all K users yields $\mathcal{O}(4|\mathcal{A}_k|K\tau_p^2+4|\mathcal{A}_k|K)$ and the iterative optimization process in GP solver incurs complexity of $\mathcal{O}(K^{3.5})$ while the complexity of setting up the constraints for GP becomes $\mathcal{O}(K^2)$. The total complexity over T iterations for the proposed method becomes $\mathcal{O}(T \cdot \left(6|\mathcal{A}_k|K\tau_p^2+6|\mathcal{A}_k|K^2+K^{3.5}+K^2+4|\mathcal{A}_k|K\right)) \approx \mathcal{O}(T \cdot K^{3.5})$.

We compare the proposed iterative pilot power allocation (IPPA) scheme with a data power allocation (DPA) scheme [13], the pilot power allocation (PPA) scheme [15], joint pilot and data power allocation (PDPA) in [18], pilot and data optimized power allocation (PDOPA) in [19], normalized estimation error-based power allocation (NEEPA) [44], and the fractional pilot power control (FPPA) scheme in [29], in which the only data power allocation is considered.

In the DPA algorithm [13], only the data power is controlled while the pilot power is set to the maximum power under the pilot power constraint. The minimum SE is maximized as the optimization objective. This method, considering $\mathcal{O}(|\mathcal{A}_k|K^2+|\mathcal{A}_k|K^2\tau_p)$ as the complexity for calculating SINR across all users, based on max-min power allocation with iterative bisection, has a total complexity of $\mathcal{O}(|\mathcal{A}_k|^2K+|\mathcal{A}_k|^2+K|\mathcal{A}_k|\log|\mathcal{A}_k|+K|\mathcal{A}_k|+T_{\text{DPA}}|\mathcal{A}_k|K^2+T_{\text{DPA}}|\mathcal{A}_k|K^2\tau_p)$ for $T_{\text{DPA}}=\log_2(\frac{t_{\max}-t_{\min}}{\kappa})$ iterations. Since this method is based on the bisection method, which results in a per-iteration complexity in the order of $\mathcal{O}(T_{\text{DPA}} \cdot K^4)$.

The PPA algorithm [15] is a scheme focused solely on controlling pilot power, while the uplink data power is set to its maximum within the data power constraint. It has an initial complexity of $\mathcal{O}(|\mathcal{A}_k|K^2)$ for computing the starting values based on algorithm 1 in [15] and follows an inner iteration (over $T_{\text{PPA}}=\log 2(\frac{t_{\max}-t_{\min}}{\kappa})$ iterations) with complexity $\mathcal{O}(|\mathcal{A}_k|K^2+|\mathcal{A}_k|K^2\tau_p)$ for each iteration. This process is repeated over T_{outer} outer iterations. Thus, the final complexity of the PPA method is $\mathcal{O}(|\mathcal{A}_k|^2K+|\mathcal{A}_k|^2+K|\mathcal{A}_k|\log|\mathcal{A}_k|+K|\mathcal{A}_k|+|\mathcal{A}_k|K^2+T_{\text{outer}}T_{\text{PPA}}|\mathcal{A}_k|K^2+|\mathcal{A}_k|K^2\tau_p)$. Although the primary goal of this method is to minimize channel estimation error, it does not adjust the data power in response to changes in pilot power. The solution from the PPA technique entails solving a convex optimization problem followed by applying the bisection method, resulting in a per-iteration complexity of $\mathcal{O}(T_{\text{outer}} \cdot T_{\text{PPA}} \cdot K^4)$.

As an example to show the computational complexity of the proposed method and other compared methods, we ran all algorithms using MATLAB 2024a on a Windows 11 personal computer with Intel(R) Xeon(R) w7-2475X,2592 MHz, 20 Cores CPU, and 64 GB memory RAM. The results are demonstrated in Table 1. To do this properly, we closed all background processes on our computer (internet, e-mail, music, and all unrelated software) and restricted MATLAB to use a single processor at all times. Furthermore, it should be noted that these measurements have been done based on the parameters given in the simulation section.

Moreover, the computational complexity of all methods, expressed in terms of floating-point operations (FLOPs), is summarized in Table 2

TABLE 1: Computational time

Approaches	Execution time (s)
IPPA	0.0095
PPA	0.2665
DPA	0.0711
PDPA	0.0899
PDOPA	0.1348
NEEPA	0.0715

TABLE 2: Computational complexity

Methods	Computational complexity
IPPA	$\mathcal{O}(T \cdot K^{3.5})$
PPA	$\mathcal{O}(T_{\text{outer}} \cdot T_{\text{PPA}} \cdot K^4)$
DPA	$\mathcal{O}(T_{\text{DPA}} \cdot K^4)$
PDPA	$\mathcal{O}\big(\max((T_{\text{outer}} \cdot T_{\text{PPA}} \cdot 2K^{3.5}), K^4)\big)$
PDOPA	$\mathcal{O}\big(T_{\text{outer}}(\max((27K^{3.5}), 9(M+5)K^2)\big)$
NEEPA	$\mathcal{O}\big(\max(T_{\text{PPA}} \cdot 2K|\mathcal{A}_k|, T_{\text{DPA}}K^4)\big)$

Fig. 3 illustrates the computational complexity of different power allocation algorithms in terms of FLOPs versus the number of users K. It can be observed that all methods exhibit an increasing trend with K, but with significantly different growth rates.

The proposed IPPA scheme achieves the lowest complexity across all values of K. For example, at $K=100$, IPPA complexity is nearly 93% lower than the conventional PPA scheme and approximately 70% lower than PDOPA. This highlights the efficiency of IPPA in large-scale scenarios. In contrast, the PPA method suffers from extremely high complexity, reaching about 4.5×10^9 FLOPs at $K=100$. This corresponds to almost 15 times higher complexity than

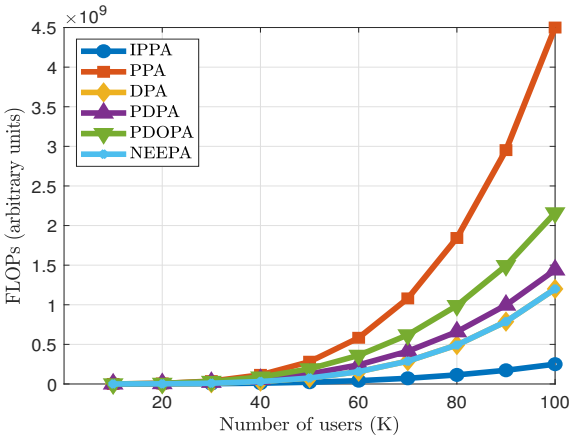

FIGURE 3: Computational complexity comparison for $M = 100$, $N = 1$, $K = 40$, and $\tau_p = 20$.

IPPA and about 200% higher than PDOPA at the same number of users. Such high growth makes PPA impractical for massive user deployments.

The DPA, PDPA, and PDOPA schemes achieve moderate complexity. At $K = 100$, PDOPA reduces complexity by around 50% compared to PPA, while DPA and PDPA further reduce it by about 65%. Nevertheless, these methods still require 3–5 times more FLOPs than IPPA, showing that while they improve scalability compared to PPA, they remain less efficient than IPPA.

Finally, the NEEPA algorithm provides complexity close to that of IPPA, achieving reductions of more than 85% compared to PPA. However, NEEPA still consumes about 30–40% more FLOPs than IPPA as K grows large. Overall, these results confirm that IPPA is the most computationally efficient solution, offering substantial savings in FLOPs.

V. Numerical Results

A. Propagation Model

This section presents numerical results to assess the performance of the proposed approach under various CFmMIMO scenarios. While many recent studies on uplink maximum ratio combining have adopted the propagation model from [13], it is important to recognize that this model is derived from the COST-Hata framework in [45], originally designed for macro-cell environments. Specifically, it assumes that APs are deployed at heights of at least 30 meters, and users are located at distances exceeding 1 km from the APs. These assumptions significantly differ from the dense, micro-cell-like deployments expected in CF-mMIMO systems. Notably, the authors of the COST-Hata model explicitly indicated that it "must not be used for micro-cells" [40]. To ensure a fair and meaningful performance evaluation, we consider both propagation models from [13] and [39], and select the most appropriate model based on comparative simulation results, as illustrated in Fig. 4.

We consider simulation setups with M APs with N antennas, and K single antenna users. Each coherence block contains $\tau_c = 200$ samples, and the total number of distributed antenna elements across the network is given by LM. Unless otherwise stated, $\tau_p = 20$ symbols are reserved for uplink pilot transmission, and each user uses its full transmit power 100 mW for pilot signaling. We performed 500-channel realizations. It is assumed that APs and users are independently and uniformly distributed within an area of 1×1 km^2, and a wrap-around technique is used to prevent boundary effects and simulate a network with an infinite area. The following three-slope propagation model was used in [13]:

$$\beta_{mk} = \begin{cases} -81.2, & d_{mk} < d_0 \\ -61.2 - 20\log_{10}\left(\frac{d_{mk}}{1}\right), & d_0 \leq d_{mk} < d_1 \\ -35.7 - 35\log_{10}\left(\frac{d_{mk}}{1}\right) + F_{mk}, & d_{mk} \geq d_1 \end{cases} \tag{30}$$

where $d_0 = 10$ m, $d_1 = 50$ m and d_{mk} is the horizontal distance between the user u and AP l (i.e., ignoring the height difference). The shadowing term $F_{mk} \sim \mathcal{CN}\left(0, 8^2\right)$ only appears when the distance is larger than 50 m and the terms are correlated as

$$\mathbb{E}\left\{F_{mk}F_{ji}\right\} = \frac{8^2}{2}\left(2^{-\delta_{ki}/100} + 2^{-\varrho_{mj}/100}\right) \tag{31}$$

where δ_{ki} is the distance between user k and user i and ϱ_{mj} is the distance between AP m and AP j. The maximum user power is 100 mW, the bandwidth is 20 MHz, and the noise power is 92 dBm.

The large-scale fading coefficient (channel gain) in [39] is modeled as:

$$\beta_{mk} = -30.5 - 36.7\log_{10}\left(\frac{d_{mk}}{1}\right) + F_{mk} \tag{32}$$

where d_{mk} is the three-dimensional distance between AP l and the user k. The APs are deployed 10 m above the plane where the users are located, which acts as the minimum distance. This model matches the 3GPP Urban Microcell model in [46]. The shadow fading is $F_{mk} \sim \mathcal{N}\left(0, 4^2\right)$ and the terms from an AP to different users are correlated as [46]

$$\mathbb{E}\left\{F_{mk}F_{ji}\right\} = \begin{cases} 4^2 2^{-\delta_{ki}/9} & m = j \\ 0 & m \neq j \end{cases} \tag{33}$$

As shown in Fig. 4, due to the limitations of the COST-Hata-based model in [13] for micro-cell scenarios—and in accordance with the recommendation in [40]—this work adopts the propagation model introduced in [39]. This model is better suited for dense and distributed AP deployments in CF-mMIMO systems and offers a more realistic assessment of system performance.

B. Simulation results

We assess the effectiveness of the proposed iterative pilot power allocation (IPPA) scheme by comparing it with a data power allocation (DPA) scheme [13], the pilot power allocation (PPA) scheme [15], joint pilot and data power

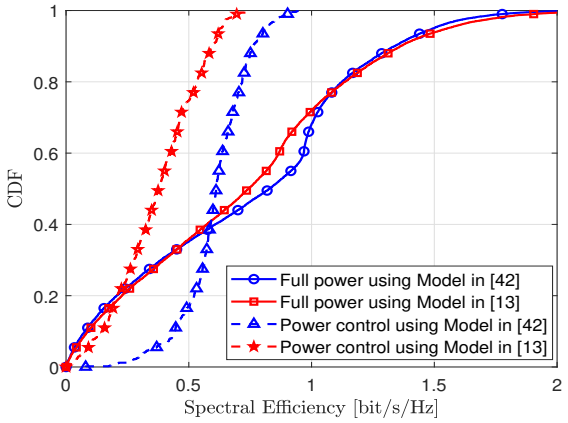

FIGURE 4: SE comparison of the proposed method in two propagation models in [13] and [39] for $M = 100$, $N = 1$, $K = 40$, and $\tau = 20$.

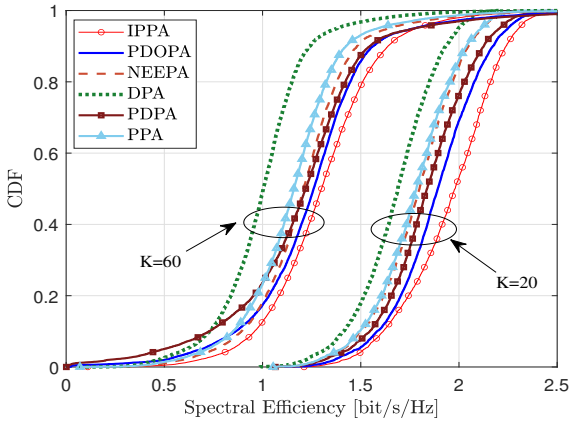

(a) CDF of SE

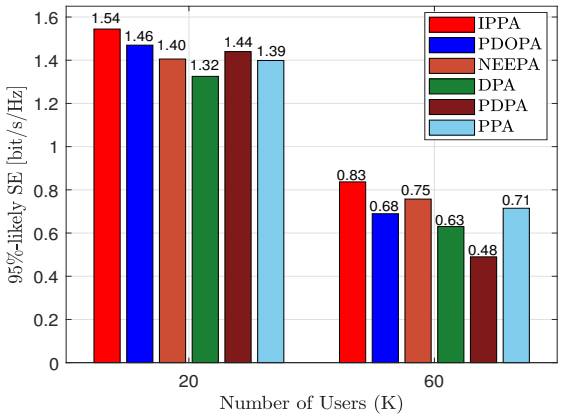

(b) 95 % likely SE

FIGURE 5: SE Performance in the case $M = 100$, $N = 3$, $K = 20$ and 60 users, and $\tau_p = 20$

allocation (PDPA) in [18], pilot and data optimized power allocation (PDOPA) in [19], normalized estimation error-based power allocation (NEEPA) [44], and the fractional pilot power control (FPPA) scheme in [29], in which the only data power allocation is considered. Note that the "NPPA" curves correspond to the cases where the users transmit with full power during the training phase. Moreover, in the proposed IPPC algorithm, we choose $\epsilon = 0.01$, and the maximum transmit budget $P_{\max}$= 100 mW.

Fig. 5 illustrates the SE performance of the proposed and benchmark algorithms for two user scenarios, $K = 20$ and $K = 60$, under the setting $M = 100$, $N = 1$, and $\tau_p = 20$.

In Fig. 5a, the cumulative distribution functions (CDFs) of SE are plotted. When the number of users is relatively small ($K = 20$), all algorithms achieve reasonably high SE, but the proposed IPPA method consistently outperforms the benchmarks across the entire distribution, yielding higher SE for both close and far users. As the system load increases to $K = 60$, the performance gap becomes more pronounced. In this dense-user scenario, conventional schemes (e.g., DPA, PDPA, PPA) suffer from degraded fairness and lower reliability, while the proposed IPPA maintains a robust SE distribution, highlighting its scalability and ability to handle larger networks effectively.

In Fig. 5b, the 95%-likely SE is presented. This metric emphasizes cell-edge user performance and fairness. For $K = 20$, the IPPA achieves the highest 95%-likely SE, followed closely by PDOPA and NEEPA, while DPA, PDPA, and PPA lag behind. When K increases to 60, all schemes experience a drop due to stronger inter-user interference and limited pilot resources. However, the IPPA retains a significant advantage, achieving the highest 95%-likely SE and ensuring reliable service even for users with poor channel conditions. The results confirm that the proposed IPPA scheme not only improves the average SE but also provides superior fairness and robustness compared to benchmark approaches, particularly in large-scale CF-mMIMO deployments with many users.

Fig. 6 presents the average SE performance as the number of users varies from 20 to 100, with fixed parameters $M = 100$, $N = 1$, and $\tau = 20$. The average SE decreases as the number of users increases for all schemes. This degradation is mainly due to stronger inter-user interference and the limited pilot resources available for accurate channel estimation, which becomes more critical in dense-user scenarios. As the number of users grows, power allocation and pilot assignment become increasingly challenging, leading to lower overall SE.

The proposed IPPA consistently outperforms all benchmark schemes across the entire range of user numbers. This improvement stems from its iterative joint pilot–data power control strategy, which dynamically adapts pilot and data powers to instantaneous channel conditions. By allocating higher pilot power to users with poor channels, IPPA improves channel estimation accuracy, and by optimizing

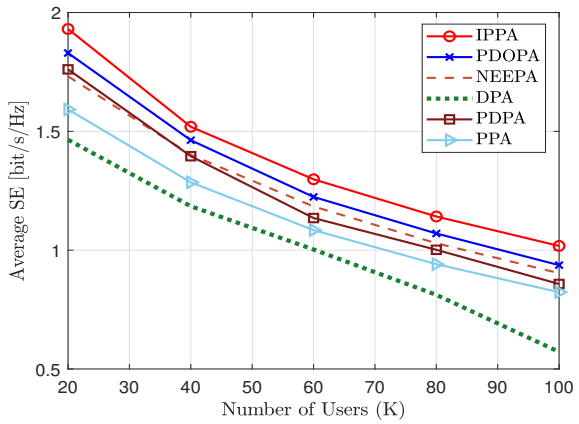

FIGURE 6: Average SE comparison with different number of users for $M = 100$, $N = 3$, and $\tau = 20$.

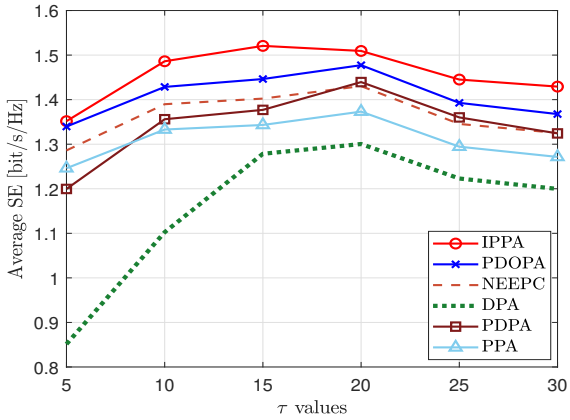

FIGURE 7: Average SE comparison with different number of pilot sequences τ for $M = 100$, $K = 40$, and $N = 3$.

data power through max–min fairness, it ensures reliable transmission while mitigating interference. This adaptability allows IPPA to sustain better performance even under heavy user loads. Although PDOPA and NEEPA also achieve relatively good performance compared to conventional methods (DPA, PDPA, PPA), they still fall short of IPPA, particularly in high-user scenarios. The reason is that they treat pilot and data power optimization separately, which limits their ability to exploit the joint structure of the problem. On the other hand, DPA, PDPA, and PPA show significantly lower average SE since they lack efficient adaptation to channel conditions and fail to maintain fairness as the network scales.

Fig. 7 illustrates the impact of the different number of pilot sequences τ, considering $M = 100$, $K = 40$, and $N = 3$. The IPPA scheme outperforms all benchmark methods for every value of τ, highlighting the effectiveness of the proposed AP-user association and iterative joint pilot-data power control. The SE performance improves when τ increases from small values. This is because longer pilot sequences reduce pilot contamination and improve channel estimation accuracy. However, beyond a certain point (e.g., τ = 10-15), further increasing τ leads to performance degradation. The reason is that allocating more resources to pilots reduces the fraction of symbols available for data transmission, thereby lowering the overall SE. This trade-off highlights the importance of selecting an appropriate pilot length to balance estimation accuracy and data throughput. On the other hand, while PDOPA and NEEPA show reasonably good performance, they remain consistently below IPPA since they treat pilot and data power optimization separately. The conventional approaches (DPA, PDPA, and PPA) perform worse due to their inability to adapt pilot power allocation to user channel conditions, which leads to poor estimation quality and weaker interference management.

Fig. 8 compares the impact of the AP configuration on the average uplink throughput of various AP selection schemes for $K = 40$ users. The proposed IPPA scheme consistently achieves the highest SE across all AP deployments, showing superior scalability when the network grows. This is because IPPA jointly adapts both the pilot and the data power in an iterative manner, which effectively mitigates pilot contamination and balances inter-user interference. As the number of APs increases, the spatial degrees of freedom improve, and IPPA is able to fully exploit these additional resources, resulting in near-linear SE growth.

In contrast, the PDOPA and NEEPA schemes also benefit from increasing APs but with lower efficiency, since their allocation rules are either partially optimized or energy-centric, limiting their ability to adapt to heterogeneous channel conditions. The conventional DPA and PPA approaches yield significantly lower SE, especially at large AP deployments, highlighting their lack of robustness in user-dense scenarios. PDPA shows competitive performance but still falls short of IPPA, as it does not dynamically re-adjust pilot and data domains in each iteration.

Another key observation is the role of AP-user association. With more APs, each user is likely served by a larger set of distributed antennas that have strong channels towards the users, improving channel hardening and reducing pathloss disparity. IPPA leverages this effect most efficiently by optimally distributing both pilot and data powers across the user domain. This demonstrates that the joint design of power allocation and AP–user association is critical for ensuring scalability in future CF-mMIMO systems.

Fig. 9 evaluates the fairness performance of the proposed and benchmark schemes from two perspectives: the CDF of the user sum rate (Fig. 9a) and Jain's fairness index (Fig. 9b). From the CDF in Fig. 9a, IPPA achieves the highest probability of offering larger sum rates compared to all other methods. This gain is attributed to its iterative nature, which balances pilot and data power in every round, thereby mitigating pilot contamination and suppressing inter-user interference more effectively. PDOPA and NEEPA also yield improved distributions compared to conventional DPA

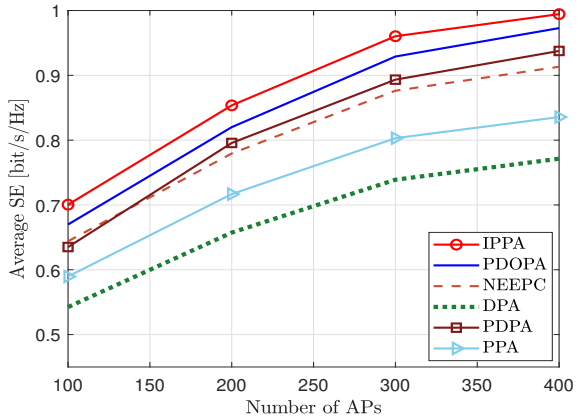

FIGURE 8: Average SE comparison with different number of APs for $K = 40$ $N = 1$, and $\tau = 20$.

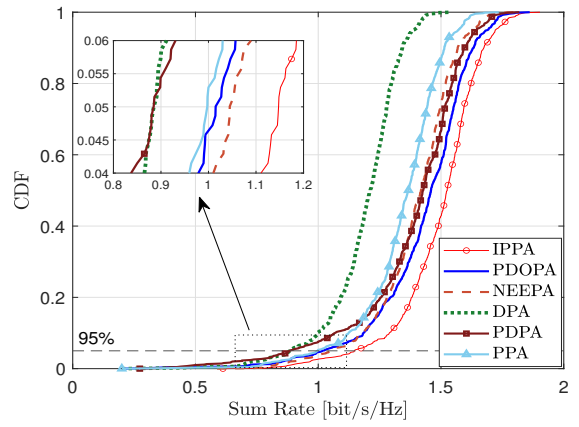

(a) CDF of Sum rate

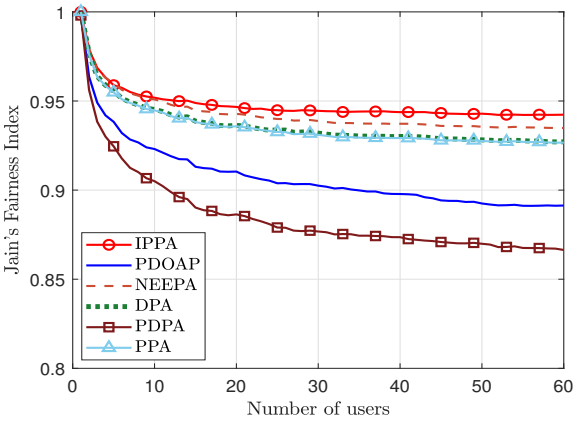

(b) Jain's fairness

FIGURE 9: Fairness performance in the case $M = 100$, $N = 3$, $K = 60$, and $\tau_p = 20$

and PPA, but their tails shift to lower rates, indicating weaker guarantees for the worst-case users. In contrast, the DPA scheme shows a sharp concentration at mid-range rates, confirming its inability to adapt to heterogeneous user conditions.

Fig. 9b provides additional insights into user fairness. The Jain's fairness index remains consistently above 0.94 for IPPA, even as the number of users increases to 60. This indicates that IPPA can maintain nearly uniform resource distribution among users while still enhancing the sum rate. PDOPA and NEEPA follow closely but gradually decline to around 0.92–0.93, reflecting a slight imbalance under high user loading. Conventional PPA and DPA methods degrade further, with fairness dropping below 0.90 for large user populations. The PDPA method performs the worst, falling below 0.87, due to its inability to strike a balance between sum-rate maximization and fairness objectives.

These results highlight two important findings. First, iterative joint allocation of pilot and data power significantly enhances both throughput and fairness, especially in dense user scenarios. Second, scalability with respect to the number of users is tightly linked to fairness guarantees: schemes like IPPA can sustain high Jain's index values, whereas conventional power allocation rapidly deteriorates as K grows.

VI. Conclusion

In this paper, we investigated a pilot and data power optimization for CF-mMIMO systems. An iterative algorithm was proposed, where pilot powers are dynamically adjusted according to the NMSE of channel estimation, while data powers are allocated using geometric programming to achieve max–min fairness. By iteratively updating pilot and data powers in response to one another, the framework ensures efficient CSI acquisition, improved interference management, and enhanced fairness among users. Furthermore, a lightweight AP–user association strategy was introduced to guarantee scalable and complete user connectivity. Simulation results confirmed that the proposed scheme significantly outperforms conventional methods in terms of both spectral efficiency and fairness, while maintaining practical scalability for large-scale CF-mMIMO deployments.

Appendix A: Proof of (29)

$$[\mathbb{E}\{\mathbf{u}_{jk}\}]_m = \mathbb{E}\{\mathbf{g}_{mk}^{\mathrm{H}}\mathbf{g}_{mj}\} \overset{(i)}{=} \mathbb{E}\{\hat{\mathbf{g}}_{mj}\hat{\mathbf{g}}_{mk}^{\mathrm{H}}\} = \begin{cases} \sqrt{p_k^{\mathrm{p}}p_j^{\mathrm{p}}}\tau_p(\beta_{mj}\theta_{mk}^{-1}\beta_{mk}) & j \in \mathcal{I}_k \\ 0 & j \notin \mathcal{I}_k \end{cases} \quad \text{(A.1)}$$

where $\mathcal{I}_k$ is the set of users that use the same pilot as user k. Since $\mathbf{g}_{mj} = \hat{\mathbf{g}}_{mj} + \tilde{\mathbf{g}}_{mj}$ and $\mathbf{g}_{mk} = \hat{\mathbf{g}}_{mk} + \tilde{\mathbf{g}}_{mk}$, then (i) follows the fact that $\tilde{\mathbf{g}}_{mj}$ (channel estimation error) and $\hat{\mathbf{g}}_{mk}$ are independent. The equality in (13) follows as

$$[\mathbf{F}_k]_{mm} = \sigma^2\mathbb{E}\{\hat{\mathbf{g}}_{mk}\hat{\mathbf{g}}_{mk}^{\mathrm{H}}\} = \sigma^2[\mathbb{E}\{\mathbf{u}_{kk}\}]_m = \sigma^2 p_k^{\mathrm{p}}\tau_p(\beta_{mk}\theta_{mk}^{-1}\beta_{mk}). \quad \text{(A.2)}$$

To compute (14), we observe that $\mathbb{E}\{[\mathbf{u}_{mj}]_m[\mathbf{u}_{mj}^*]_r\} = \mathbb{E}\{[\mathbf{u}_{mj}]_m\}\mathbb{E}\{[\mathbf{u}_{mj}^*]_r\}$ for $r \neq m$ since the the channels

of different APs are independent. Hence, it only remains to compute

$$[\mathbb{E}\{\mathbf{u}_{jk}\mathbf{u}_{jk}^{\mathrm{H}}\}]_{mm} = \mathbb{E}\left\{\hat{\mathbf{g}}_{mk}^{\mathrm{H}}\mathbf{g}_{mj}\mathbf{g}_{mj}^{\mathrm{H}}\hat{\mathbf{g}}_{mk}\right\} = \mathbb{E}\left\{\mathbf{g}_{mj}\mathbf{g}_{mj}^{\mathrm{H}}\hat{\mathbf{g}}_{mk}\hat{\mathbf{g}}_{mk}^{\mathrm{H}}\right\}. \tag{A.3}$$

If $j \notin \mathcal{I}_k$, we can utilize the independence of $\hat{\mathbf{g}}_{mk}$ and $\mathbf{g}_{mj}$ to obtain

$$\mathbb{E}\left\{\mathbf{g}_{mj}\mathbf{g}_{mj}^{\mathrm{H}}\hat{\mathbf{g}}_{mk}\hat{\mathbf{g}}_{mk}^{\mathrm{H}}\right\} = \mathbb{E}\left\{\mathbf{g}_{mj}\mathbf{g}_{mj}^{\mathrm{H}}\right\}\mathbb{E}\left\{\hat{\mathbf{g}}_{mk}\hat{\mathbf{g}}_{mk}^{\mathrm{H}}\right\} = p_k^{\mathrm{p}}\tau_p\beta_{mj}\beta_{mk}\theta_{mk}^{-1}\beta_{mk}. \tag{A.4}$$

If $j \in \mathcal{I}_k$, we can write that

$$\mathbb{E}\left\{\mathbf{g}_{mj}\mathbf{g}_{mj}^{\mathrm{H}}\hat{\mathbf{g}}_{mk}\hat{\mathbf{g}}_{mk}^{\mathrm{H}}\right\} \overset{(ii)}{=} \mathbb{E}\{\hat{\mathbf{g}}_{mj}\hat{\mathbf{g}}_{mj}^{\mathrm{H}}\hat{\mathbf{g}}_{mk}\hat{\mathbf{g}}_{mk}^{\mathrm{H}}\} + \mathbb{E}\{\tilde{\mathbf{g}}_{mj}\tilde{\mathbf{g}}_{mj}^{\mathrm{H}}\hat{\mathbf{g}}_{mk}\hat{\mathbf{g}}_{mk}^{\mathrm{H}}\}, \tag{A.5}$$

(*ii*) follows separating $\mathbf{g}_{mj}$ into its estimate ($\hat{\mathbf{g}}_{mk}$) and estimation error ($\tilde{\mathbf{g}}_{mk}$). The first term is completed by utilizing the results from (Eq. (4.18), [38]) in which $\hat{\mathbf{g}}_{mj}$ is estimated as

$$\hat{\mathbf{g}}_{mj} = \sqrt{\frac{p_j^{\mathrm{p}}}{p_k^{\mathrm{p}}}}\beta_{mj}\beta_{mk}^{-1}\hat{\mathbf{g}}_{mk}, \tag{A.6}$$

and

$$\begin{aligned}
&\mathbb{E}\{\hat{\mathbf{g}}_{mj}\hat{\mathbf{g}}_{mj}^{\mathrm{H}}\hat{\mathbf{g}}_{mk}\hat{\mathbf{g}}_{mk}^{\mathrm{H}}\} \\
&= \frac{p_j^{\mathrm{p}}}{p_k^{\mathrm{p}}}\mathbb{E}\{\beta_{mj}\beta_{mk}^{-1}\hat{\mathbf{g}}_{mk}\hat{\mathbf{g}}_{mk}^{\mathrm{H}}\beta_{mk}^{-1}\beta_{mj}\hat{\mathbf{g}}_{mk}\hat{\mathbf{g}}_{mk}^{\mathrm{H}}\} \\
&= \frac{p_j^{\mathrm{p}}}{p_k^{\mathrm{p}}}\mathbb{E}\{|\hat{\mathbf{g}}_{mk}\beta_{mj}\beta_{mk}^{-1}\hat{\mathbf{g}}_{mk}^{-1}|^2\} \\
&= p_k^{\mathrm{p}}p_j^{\mathrm{p}}|\tau_p\beta_{mj}\theta_{mk}^{-1}\beta_{mk}|^2 + p_k^{\mathrm{p}}\tau_p\big((\beta_{mj}-\gamma_{mj})\beta_{mk}\theta_{mk}^{-1}\beta_{mk}\big),
\end{aligned} \tag{A.7}$$

where $\gamma_{mj} = \beta_{mj} - p_j^{\mathrm{p}}\tau_p\beta_{mj}\theta_{mk}^{-1}\beta_{mj}$.
Also, the second term becomes

$$\mathbb{E}\{\tilde{\mathbf{g}}_{mj}\tilde{\mathbf{g}}_{mj}^{\mathrm{H}}\hat{\mathbf{g}}_{mk}\hat{\mathbf{g}}_{mk}^{\mathrm{H}}\} = p_k^{\mathrm{p}}\tau_p\gamma_{mj}\beta_{mk}\theta_{mk}^{-1}\beta_{mk}. \tag{A.8}$$

By combining these two terms, we obtain (14). Replacing (A.1),(VI), and (A.3) into (11) we will achieve (29).

Appendix B

The standard form of GP is defined as follows [34]:

$$\begin{aligned}
&\min \ \ f_0(\mathbf{x}), \\
&\text{s.t.} \quad f_j(\mathbf{x}) \le 1, \ \ j = 1, \cdots, m, \\
&\qquad q_j(\mathbf{x}) = 1, \ \ j = 1, \cdots, c,
\end{aligned}$$

where f_0 and f_1 are posynomial and q_i are monomial functions. Moreover, $x = \{x_1, \cdots x_n\}$ represent the optimization variables. The SINR constraint in (29) can be written as Numerator (Desired Signal Power) as:

$$(No)_k = N\tau_p p_k^{\mathrm{d}}p_k^{\mathrm{p}}\sum_{m=1}^{M}\beta_{mk}^2\theta_{mk}^{-1}. \tag{B.1}$$

and denominator (interference plus noise) term as:

$$(De)_k = \sum_{l\in\mathcal{A}_k}\Big(N\tau_p\sum_{\substack{i\in\mathcal{S}_k \\ i\neq k}}p_i^{\mathrm{d}}p_i^{\mathrm{p}}\beta_{mi}^2\theta_m^{-1} + \sum_{i=1}^{K}p_i^{\mathrm{d}}\beta_{mi}\Big) + \sigma^2. \tag{B.2}$$

Thus, we can rewrite the SINR as:

$$\mathrm{SINR}_k = \frac{(No)_k}{(De)_k}. \tag{B.3}$$

We check if the numerator and denominator can be written in the posynomial form. In (B.1), since N, τ_p, β_{mk}, and θ_{mk} are constants, we have:

$$(No)_k = p_k^{\mathrm{d}}p_k^{\mathrm{p}}\cdot(\text{constant}). \tag{B.4}$$

This is a monomial, which is compatible with GP.
The denominator, De_k, is composed of several terms:

1- *Inter-user interference term:* This is given by $N\tau_p\sum_{i\neq k}p_i^{\mathrm{d}}p_i^{\mathrm{p}}\beta_{mi}^2\theta_{mk}^{-1}$. It represents a sum over all users $i \neq k$, where each term is a product of p_i^{d}, p_i^{p}, and a constant, making it a monomial.
2- *Intra-user interference term:* This is expressed as $\sum_{i=1}^{K}p_i^{\mathrm{d}}\beta_{mi}$. Here, each term is a product of p_i^{d} and a constant, which also qualifies as a monomial.
3- *Noise term:* Represented by σ^2, this is simply a constant.

As a result, (De_k) is a sum of these monomials, which collectively form a posynomial. Since posynomials are compatible with GP, this structure aligns well with the requirements for GP-based optimization.

REFERENCES

[1] T. L. Marzetta, "Noncooperative cellular wireless with unlimited numbers of base station antennas," *IEEE Transactions on Wireless Communications*, vol. 9, no. 11, pp. 3590–3600, 2010.
[2] E. G. Larsson, O. Edfors, F. Tufvesson, and T. L. Marzetta, "Massive MIMO for next generation wireless systems," *IEEE Communications Magazine*, vol. 52, no. 2, pp. 186–195, 2014.
[3] S. Parkvall, E. Dahlman, A. Furuskar, and M. Frenne, "NR: The new 5G radio access technology," *IEEE Communications Standards Magazine*, vol. 1, no. 4, pp. 24–30, 2017.
[4] S. Buzzi, I. Chih-Lin, T. E. Klein, H. V. Poor, C. Yang, and A. Zappone, "A survey of energy-efficient techniques for 5G networks and challenges ahead," *IEEE Journal on Selected Areas in Communications*, vol. 34, no. 4, pp. 697–709, 2016.
[5] W. Saad, M. Bennis, and M. Chen, "A vision of 6G wireless systems: Applications, trends, technologies, and open research problems," *IEEE Network*, vol. 34, no. 3, pp. 134–142, 2019.
[6] H. Q. Ngo, E. G. Larsson, and T. L. Marzetta, "Energy and spectral efficiency of very large multiuser MIMO systems," *IEEE Transactions on Communications*, vol. 61, no. 4, pp. 1436–1449, 2013.
[7] M. Bashar, K. Cumanan, A. G. Burr, M. Debbah, and H. Q. Ngo, "On the uplink max-min SINR of cell-free massive MIMO systems," *IEEE Transactions on Wireless Communications*, vol. 18, no. 4, pp. 2021–2036, 2019.
[8] Z. Chu, P. Xiao, C. H. Foh, D. Mi, K. Cumanan, and A. G. Burr, "Joint ITS-and IRS-assisted cell-free networks," *IEEE wireless communications letters*, vol. 13, no. 3, pp. 859–863, 2023.
[9] B. Chong and H. Lu, "Statistical QoS provisioning for URLLC in cell-free massive MIMO systems," *IEEE Transactions on Communications*, vol. 72, no. 12, pp. 7650–7663, 2024.

[10] H. V. Cheng, E. Björnson, and E. G. Larsson, "Optimal pilot and payload power control in single-cell massive MIMO systems," *IEEE Transactions on Signal Processing*, vol. 65, no. 9, pp. 2363–2378, 2016.

[11] A. Ghazanfari, E. Björnson, and E. G. Larsson, "Optimized power control for massive MIMO with underlaid D2D communications," *IEEE Transactions on Communications*, vol. 67, no. 4, pp. 2763–2778, 2018.

[12] T. Van Chien, T. N. Canh, E. Björnson, and E. G. Larsson, "Power control in cellular massive MIMO with varying user activity: A deep learning solution," *IEEE Transactions on Wireless Communications*, vol. 19, no. 9, pp. 5732–5748, 2020.

[13] H. Q. Ngo, A. Ashikhmin, H. Yang, E. G. Larsson, and T. L. Marzetta, "Cell-free massive MIMO versus small cells," *IEEE Transactions on Wireless Communications*, vol. 16, no. 3, pp. 1834–1850, 2017.

[14] T. H. Nguyen, T. K. Nguyen, H. D. Han *et al.*, "Optimal power control and load balancing for uplink cell-free multi-user massive MIMO," *IEEE Access*, vol. 6, pp. 14 462–14 473, 2018.

[15] T. C. Mai, H. Q. Ngo, M. Egan, and T. Q. Duong, "Pilot power control for cell-free massive MIMO," *IEEE Transactions on Vehicular Technology*, vol. 67, no. 11, pp. 11 264–11 268, 2018.

[16] H. Masoumi and M. J. Emadi, "Joint pilot and data power control in cell-free massive MIMO system," in *2018 Fifth International Conference on Millimeter-Wave and Terahertz Technologies (mmWatt)*. IEEE, 2018, pp. 34–37.

[17] T. C. Mai, H. Q. Ngo, and L.-N. Tran, "Design of pilots and power control in the cell-free massive MIMO uplink," in *2020 54th Asilomar Conference on Signals, Systems, and Computers*. IEEE, 2020, pp. 831–835.

[18] I. M. Braga, R. P. Antonioli, G. Fodor, Y. C. Silva, and W. C. Freitas, "Joint pilot and data power control optimization in the uplink of user-centric cell-free systems," *IEEE Communications Letters*, vol. 26, no. 2, pp. 399–403, 2021.

[19] G. Liu, H. Deng, X. Qian, W. Zhang, and H. Dong, "Joint pilot and data power control for cell-free massive MIMO IoT systems," *IEEE Sensors Journal*, vol. 22, no. 24, pp. 24 647–24 657, 2022.

[20] N. Rajapaksha, N. Rajatheva, and M. Latva-Aho, "Deep learning-based joint pilot and data power control in cell-free massive MIMO networks," in *2024 IEEE 100th Vehicular Technology Conference (VTC2024-Fall)*. IEEE, 2024, pp. 1–6.

[21] N. Rajapaksha, K. S. Manosha, N. Rajatheva, and M. Latva-Aho, "Deep learning-based power control for cell-free massive MIMO networks," in *ICC 2021-IEEE International Conference on Communications*. IEEE, 2021, pp. 1–7.

[22] Y. Hao, J. Xin, W. Tao, S. Tao, L. Yu-xiang, and W. Hao, "Pilot allocation algorithm based on k-means clustering in cell-free massive MIMO systems," in *2020 IEEE 6th International Conference on Computer and Communications (ICCC)*. IEEE, 2020, pp. 608–611.

[23] C. D'Andrea, A. Zappone, S. Buzzi, and M. Debbah, "Uplink power control in cell-free massive MIMO via deep learning," in *2019 IEEE 8th International workshop on computational advances in multi-sensor adaptive processing (CAMSAP)*. IEEE, 2019, pp. 554–558.

[24] Y. Zhao, I. G. Niemegeers, and S. H. De Groot, "Power allocation in cell-free massive MIMO: A deep learning method," *IEEE Access*, vol. 8, pp. 87 185–87 200, 2020.

[25] Q.-S. Nguyen, X.-T. Dang, and O.-S. Shin, "Joint pilot and data power optimization in cell-free massive MIMO systems using heterogeneous graph convolutional network," in *2024 Tenth International Conference on Communications and Electronics (ICCE)*. IEEE, 2024, pp. 735–740.

[26] Z. Duan and F. Zhao, "Pilot allocation and data power optimization based on access point selection in cell-free massive MIMO," *Wireless Communications and Mobile Computing*, vol. 2022, no. 1, p. 4044783, 2022.

[27] S. Jamshidi, O. Mahdiyar, A. Ghaedi *et al.*, "Optimal pilot and data power allocation in the cell-free massive MIMO systems," 2022.

[28] Y. Zhang, J. Zhang, S. Buzzi, H. Xiao, and B. Ai, "Unsupervised deep learning for power control of cell-free massive MIMO systems," *IEEE Transactions on Vehicular Technology*, vol. 72, no. 7, pp. 9585–9590, 2023.

[29] R. Nikbakht and A. Lozano, "Uplink fractional power control for cell-free wireless networks," in *ICC 2019-2019 IEEE International Conference on Communications (ICC)*. IEEE, 2019, pp. 1–5.

[30] S. Chakraborty, Ö. T. Demir, E. Björnson, and P. Giselsson, "Efficient downlink power allocation algorithms for cell-free massive MIMO systems," *IEEE Open Journal of the Communications Society*, vol. 2, pp. 168–186, 2020.

[31] S. Mohammadzadeh, S. Mashdour, R. C. de Lamare, K. Cumanan, and C. Li, "Association of access points and users and power allocation for cell-free massive MIMO systems," in *2025 IEEE 26th International Workshop on Signal Processing and Artificial Intelligence for Wireless Communications (SPAWC)*. IEEE, 2025, pp. 1–5.

[32] M. Zaher, Ö. T. Demir, E. Björnson, and M. Petrova, "Learning-based downlink power allocation in cell-free massive MIMO systems," *IEEE Transactions on Wireless Communications*, vol. 22, no. 1, pp. 174–188, 2022.

[33] L. Salaün, H. Yang, S. Mishra, and C. S. Chen, "A GNN approach for cell-free massive MIMO," in *GLOBECOM 2022-2022 IEEE Global Communications Conference*. IEEE, 2022, pp. 3053–3058.

[34] M. Chiang, C. W. Tan, D. P. Palomar, D. O'neill, and D. Julian, "Power control by geometric programming," *IEEE Transactions on Wireless Communications*, vol. 6, no. 7, pp. 2640–2651, 2007.

[35] S. Boyd, S.-J. Kim, L. Vandenberghe, and A. Hassibi, "A tutorial on geometric programming," *Optimization and Engineering*, vol. 8, pp. 67–127, 2007.

[36] L. Sanguinetti, M. Morelli, and L. Marchetti, "A random access algorithm for lte systems," *Transactions on Emerging Telecommunications Technologies*, vol. 24, no. 1, pp. 49–58, 2013.

[37] E. Björnson, J. Hoydis, L. Sanguinetti *et al.*, "Massive MIMO networks: Spectral, energy, and hardware efficiency," *Foundations and Trends® in Signal Processing*, vol. 11, no. 3-4, pp. 154–655, 2017.

[38] Ö. T. Demir, E. Björnson, L. Sanguinetti *et al.*, "Foundations of user-centric cell-free massive MIMO," *Foundations and Trends® in Signal Processing*, vol. 14, no. 3-4, pp. 162–472, 2021.

[39] E. Björnson and L. Sanguinetti, "Scalable cell-free massive MIMO systems," *IEEE Transactions on Communications*, vol. 68, no. 7, pp. 4247–4261, 2020.

[40] ——, "Making cell-free massive MIMO competitive with mmse processing and centralized implementation," *IEEE Transactions on Wireless Communications*, vol. 19, no. 1, pp. 77–90, 2019.

[41] T. L. Marzetta, E. G. Larsson, H. Yang, and H. Q. Ngo, *Fundamentals of massive MIMO*. Cambridge University Press, 2016.

[42] S. P. Boyd and L. Vandenberghe, *Convex optimization*. Cambridge university press, 2004.

[43] M. Grant, S. Boyd, and Y. Ye, "CVX: Matlab software for disciplined convex programming (web page and software)," http://cvxr.com/cvx, 2009, [Online; accessed 2025-10-15].

[44] M. Sarker and A. O. Fapojuwo, "Pilot power allocation scheme for user-centric cell-free massive MIMO systems," in *2023 IEEE 20th Consumer Communications & Networking Conference (CCNC)*. IEEE, 2023, pp. 763–768.

[45] P. E. Mogensen and J. Wigard, "Cost action 231: Digital mobile radio towards future generation system, final report." in *Section 5.2: On antenna and frequency diversity in GSM. Section 5.3: Capacity study of frequency hopping GSM network*, 1999.

[46] "Further Advancements for E-UTRA Physical Layer Aspects (Release 9)," 3rd Generation Partnership Project (3GPP), 3GPP Technical Specification TS 36.814, 2017, version 9.2.0.

Saeed Mohammadzadeh embarked on his academic journey at the University of Shahid Beheshti, where he earned his Bachelor of Science degree. Building on this foundation, he pursued advanced studies and obtained his Master's degree in 2014, followed by a Ph.D. degree in 2019, both from the prestigious Eastern Mediterranean University. He served as a Postdoctoral Researcher at the esteemed University of São Paulo. In this role, he continued to push the boundaries of knowledge in the realm of Electrical Engineering and signal processing. He is the reviewer of a number of high-prestige journals in the field of signal processing and communications. His research interests are both diverse and profound, encompassing a range of topics including array signal processing, adaptive beamforming, cell-free massive MIMO, machine learning, integrated sensing and communication systems (ISAC),

and NOMA. He currently serves as a research fellow at the Department of Electronics at the University of York.

Mostafa Rhamani Ghourtani received the B.Sc. degree in electrical engineering from Shiraz University, Iran, in 2009, the M.Sc. degree in communication systems engineering from Tarbiat Modares University, Tehran, Iran, in 2012, and the Ph.D. degree in communication systems engineering from the Shiraz University of Technology, Iran, in 2023. He is currently a Postdoctoral Researcher with the University of York. His research interests focus on wireless communication systems, including MIMO and cell-free massive MIMO, Open RAN, physical-layer network coding, and the application of machine learning and deep reinforcement learning in communications.

Kanapathippillai Cumanan (M'10, SM'19) Dr. Cumanan received the BSc degree with first class honors in electrical and electronic engineering from the University of Peradeniya, Sri Lanka, in 2006 and subsequently obtained his PhD degree in signal processing for wireless communications from Loughborough University, Loughborough, UK, in 2009. He is currently a Professor of Wireless Communications at the School of Physics, Engineering and Technology, University of York, UK. Prior to this, he served as an Assistant Lecturer at the Department of Electrical and Electronic Engineering, University of Peradeniya, Sri Lanka, from January 2006 to August 2006. Between January 2010 and March 2012, he held a Research Associate position at Loughborough University, UK, followed by a similar role at Newcastle University, Newcastle upon Tyne, UK, from March 2012 to November 2014. He joined as a lecturer at the University of York, UK, in November 2014. In 2011, he was also an Academic Visitor at the Department of Electrical and Computer Engineering, National University of Singapore. His research interests include non-orthogonal multiple access (NOMA), cell-free massive MIMO, physical layer security, cognitive radio networks, convex optimization techniques, and resource allocation techniques. He has published more than 100 journal articles and conference papers, which have collectively received more than 5000 Google Scholar citations. Dr. Cumanan was the recipient of an overseas research student award scheme (ORSAS) from Cardiff University, Wales, UK, where he was a research student between September 2006 and July 2007.

Alister Burr was born in London, U.K., in 1957. He received the B.Sc. degree in electronic engineering from the University of Southampton, U.K., in 1979 and the Ph.D. degree from the University of Bristol in 1984. From 1975 to 1985, he worked with Thorn-EMI Central Research Laboratories in London. In 1985, he joined the Department of Electronics (currently part of the School of Physics, Engineering and Technology), University of York, U.K, where he has been Professor of Communications since 2000. He has published more than 300 papers in refereed international conferences and journals, and is the author of "Modulation and Coding for Wireless Communications" (published by Prentice-Hall/PHEI), and co-author of "Wireless Physical-Layer Network Coding" (Cambridge University Press, 2018). He has also given more than 20 invited presentations, including six keynote presentations. His research interests are in wireless communication systems, including MIMO and cell-free massive MIMO, Open RAN, physical-layer network coding, and iterative detection and decoding techniques. In 1999, he was awarded a Senior Research Fellowship by the U.K. Royal Society, and he received the J. Langham Thompson Premium from the Institution of Electrical Engineers in 2002. He has been a Co-Chair, working group 2, of a series of European COST programmes, including currently CA20120 INTERACT, and has also served as an Associate Editor for IEEE COMMUNICATIONS LETTERS, a Workshops Chair for IEEE ICC 2016, and a TPC Co-Chair for PIMRC 2018 and 2020.

Pei Xiao is currently a Professor in wireless communications with the Institute for Communication Systems (ICS), University of Surrey. He is also the Technical Manager of 5GIC/6GIC, leading the research team in the new physical layer work area and coordinating/supervising research activities across all the work areas (https://www.surrey.ac.uk/institute-communicationsystems/5g-6g- nnovationcentre). Prior to this, he was with Newcastle University and Queen's University of Belfast. He also held positions with Nokia Networks, Finland. He has published extensively in the fields of communication theory, RF, and antenna design, and signal processing for wireless communications; and is an inventor of over 15 recent patents addressing bottleneck problems in 5G/6G systems.